ETH zürich

Semester Project

Estimating weak lensing convergence from galaxy sizes

Noah Kirchhoff
nkirchhoff@ethz.ch

May 26, 2025

Supervisors:
Prof. Dr. Alexandre Refregier
Veronika Oehl

Cosmology Group
Institute for Particle Physics and Astrophysics
Department of Physics, D-PHYS
ETH Zürich

I would like to thank Prof. Dr. Alexandre Refregier for the opportunity to work in his group and making this project possible.
I also want to thank Veronika for supervising my work, for always helping me whenever I got stuck and for the endless ideas of how to make things work and how to expand this project.

Abstract

In this project we find a weak lensing convergence estimator and use it to recover several summary statistics of the convergence map, including the power spectrum. To obtain such an estimator we use a simulated galaxy catalogue with $30,000,000$ galaxies over an area of 1000deg^2. The most promising estimators are based on the ideas of using the means of galaxy sizes and the Wasserstein distance between the galaxy size distributions of single areas and the whole catalogue. For both estimators, we are able to recover the skewness of the convergence distribution within a 1σ neigbourhood of the original convergence distribution in that area as well as a power spectrum that aligns within 1σ with the power spectrum of the original convergence map in the covered section of the catalogue. The recovered standard deviation as well as the mean of the convergence distribution are within a 2σ and 1σ range respectively for the estimator based on the Wasserstein distance and they do not align for the estimator based on the means.

Contents

1 Introduction

Gravitational lensing defines the phenomenon of the bending of the path of light around a mass distribution, which is described by Einsteins theory of general relativity. The first proof of gravitational lensing was also the first proof of general relativity, where the deflection of light caused by the sun was measured [3]. Back then it was unclear if the phenomenon would have a big impact on astrophysics, but in 1979 the first gravitational lens apart from the sun was found by the observation of a twin quasar, which turned out to be the same object that appeared as two images [8]. Most of these deflections are so weak, that it is impossible to detect them by only using one source. This regime is called the weak-lensing regime and allows us to statistically measure the distribution of foreground masses using the light of background sources. In particular, gravitational lensing can be measured using two effects: The change in size and the change in shape. The shear – change in shape – has been studied extensively in the past and measured at high precision [9], but the convergence – change in size – on the other hand not as much. In this project we focus on finding a robust way to estimate the convergence using simulated galaxy sizes. This study of the convergence can lead to a more complete way to investigate large-scale structures, i.e. map the distribution of dark matter, and to a better understanding of methods and systematics of weak lensing.

2 Theory

As already mentioned in the introduction, the effect of weak gravitational lensing can be split into two parts: The change of shape and size, also called the shear and the convergence respectively. A more detailed explanation about this split up can be found in [2]. In this project we will focus on the convergence κ, which is a measure for the size change of a light source. Put into a formula [7], this means that the lensed angular size θ' depends to first order on the intrinsic angular size θ via:

$$\theta' = (1 + \kappa)\theta \tag{1}$$

From theory, we can predict the statistical distribution of the convergence, which we will then use to simulate a convergence field. The power spectrum describes the correlation of the convergence κ between two points on the sphere and completely characterizes a Gaussian field, in this case the convergence field. The typical correlation length – the radius in which the value of two points of the convergence map are correlated – is much larger than the average distance between galaxies. This means that galaxies near to each other should experience a similar effect from gravitational lensing and the convergence in particular.
The convergence power spectrum C_ℓ^κ, using the Limber-approximation [6], is given by:

$$C_\ell^\kappa = \frac{9}{4}\frac{H_0^4}{c^4}\Omega_{m,0}^2 \int_0^{\chi(z)} d\chi' \left(\frac{\chi - \chi'}{a\chi}\right)^2 P_\delta\left(k = \frac{\ell}{\chi'}\right) \tag{2}$$

where χ is the comoving radial distance, H_0 the Hubble constant, c the speed of light, $\Omega_{m,0}$ the fractional energy density of matter, P_δ the density power spectrum, a the scale factor and ℓ the angular wave number or multipole moment. The power spectrum shown in equation 2 is the power spectrum for a single galaxy with a redshift z. For applications, redshift distributions are used for the source galaxies. A derivation and a more detailed explanation of this power spectrum can be found in [9]. Since the power spectrum is

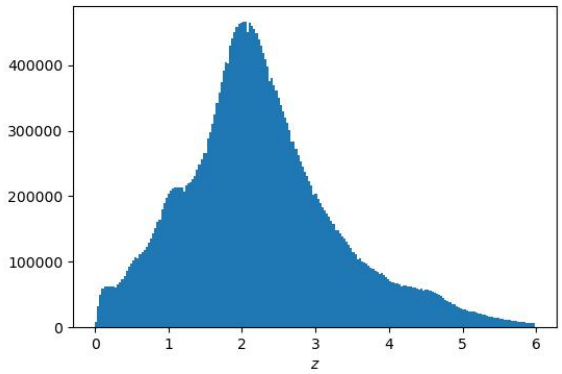

Figure 1: The redshift distribution of the largest galaxy catalogue used in the project.

dependent on cosmological parameters, measuring the power spectrum is an indirect measurement of these parameters.

The power spectrum also allows us to compute the standard deviation of the κ distribution via :

$$\sigma_\kappa^2 = \sum_{\ell=0}^{\infty} \frac{2\ell+1}{4\pi} C_\ell^\kappa \tag{3}$$

3 Modelling

3.1 Galaxy catalogue

Since points close to each other have a similar κ-value, we will divide the galaxies and also the convergence map into pixels, which we assume to have the same κ-value. We use these pixels to derive an estimator for the convergence κ based on the lensed angular sizes θ', for which we assume not to know the actual convergence of each pixel.

The simulation of the galaxies used in the project follows the procedure of [4]. The absolute magnitudes of the galaxies are sampled from a Schechter luminosity function

$$\phi(z, M) = \frac{2}{5} \ln(10) \phi^*(z) 10^{\frac{2}{5}(M^*(z)-M)(\alpha+1)} \exp\left(-10^{\frac{2}{5}(M^*(z)-M)}\right) \tag{4}$$

where ϕ^* and M^* are functions of the redshift z and α is free parameter. For a sampled absolute magnitude M the half light radius r_{50} – the radius at which half of the total light of the galaxy is emitted – is then sampled from log-normal distribution. Since the surface brightness profile of a galaxy is well described by exponential functions, we can use the half light radius as a measure of the size of the galaxy. We split the catalogue up into five redshift bins using a Gaussian mixture model and use the bin with the largest mean redshift for this project. The redshift distribution of this bin is shown in fig. 1.

Over the course of the project we used different catalogues with different sizes, the largest with an approximate galaxy count of $30,000,000$ over 1000deg^2.

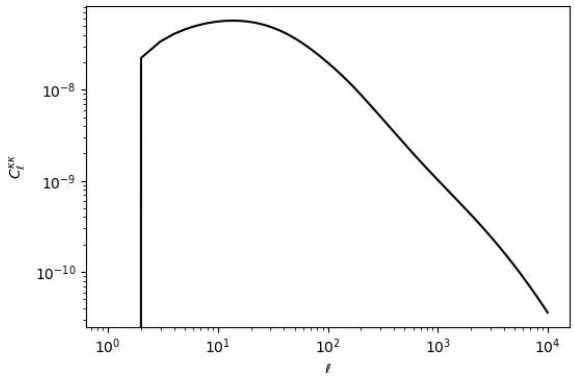

Figure 2: Convergence power spectrum used to generate the convergence map.

3.2 Convergence maps

The power spectrum using a source redshift distribution corresponding to the redshift distribution of our galaxy catalogue is shown in figure 2.
We create Gaussian convergence maps using the healpy python package, in particular the healpy synfast method [10]. In most cases we use a convergence map with an nside – the healpy parameter for the resolution – of 64, which is equivalent to a resolution of roughly 0.84deg^2 per pixel.
To get the lensed angular sizes of the galaxies in the catalogue, we apply equation 1 to the unlensed galaxy sizes. We assign each galaxy to a κ-pixel corresponding to its position in the sky.

4 Methodology

4.1 Different Convergence Estimators

In this project, we will look at multiple methods of how to construct such a convergence estimator. All estimators are based on the idea of comparing the galaxy size distribution in a single pixel to the overall size distribution, which can be seen in figure 3.
The first idea is to use statistical averages, namely the mean, median and mode. For this we will take the average of the lensed sizes of all galaxies in a single pixel. Since all galaxy sizes in the pixel have been magnified the same way, taking the average should result in a linear relation between the mean of the size in the pixel and the convergence κ in the pixel.
Another way to relate the sizes to the convergence is to compare the size distribution of a pixel to the size distribution of the whole catalogue directly. A way to do this is using optimal transport, also called the Wasserstein distance. To understand the concept more easily, one can image two piles of earth. The Wasserstein distance quantifies the amount of work needed to transform one pile into the other, which is the reason it is also called the earth mover's distance. It works similarly in this case, it describes the similarity of the two size distributions. A more thorough explanation can be found in [4]. In this project we use the W1 distance in particular, which is implemented in python using the POT python package [5].

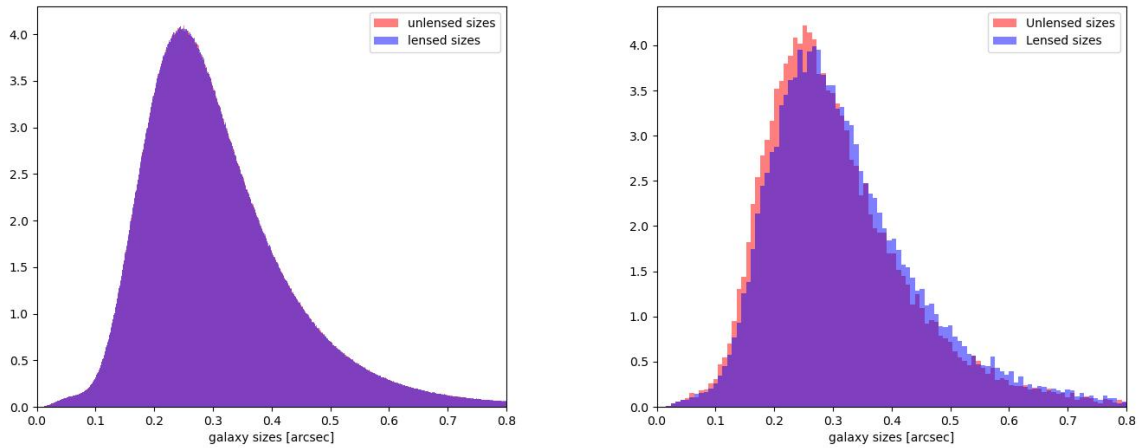

Figure 3: The unlensed (red) and lensed (blue) size distributions. We show the full catalogue (left panel) and the galaxies contained in a single pixel (right panel). For the lensing of the sizes in the pixel a κ-value of 0.05 is used.

4.2 Convergence recovery

To recover the κ-values of the original convergence map we consider two different methods: Recovery per pixel and pointwise recovery. These are explained in more detail in the next two sections.

4.2.1 Convergence recovery per pixel

In the first method we use the estimator to calculate one κ-value per pixel. This means that we need to know the pixelsize and boundaries of the original convergence map. These κ-values are then plugged into a map with the known pixelsize. Since we are only able to recover a part of the sky – the area our galaxy catalogue covers – our convergence map also contains not the whole sky but only this part, the rest is left blank.

4.2.2 Pointwise κ recovery

As already mentioned, a problem with the first method is that the pixelsize and boundaries of the original convergence map needs to be known to recover the κ-value for each pixel separately. In reality we of course cannot assume anything about this pixelsize since the real convergence map is continuous as it depends on the distribution of matter. To overcome this technical issue we recover the κ-value for each galaxy individually. We do this by calculating the κ-value from the set of galaxies that are in a set radius around the galaxy we want to calculate κ for. The radius is set such that on average enough galaxies are contained within this radius and the radius is chosen such that the unlensed mean is similar to the mean of the catalogue. To compare the two methods we can recover the pixels by averaging over the calculated κ-values of all galaxies in the pixel. The generation of the convergence map then follows the same procedure as in the first method. A sketch of this method can be seen in figure 4.

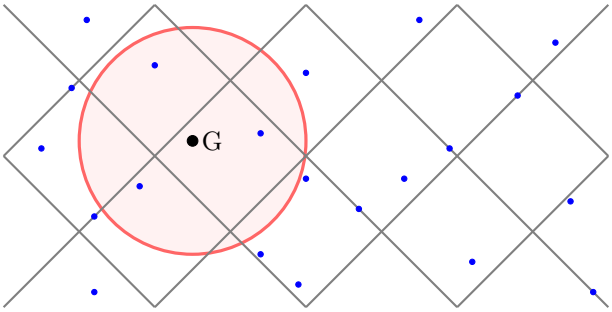

Figure 4: Sketch of the pointwise recovery method. To calculate the κ-value of the galaxy G the sizes of all galaxies (the blue dots) inside a radius (the red circle) are considered.

4.3 Recovery of summary statistics

Even if the pixel values do not match perfectly, the underlying statistics might still be recovered correctly and therefore also the cosmology. This is why we run statistical tests, for example the mean, standard deviation or the two-point function.

The two-point function, in this case the power spectrum in spherical harmonic space, is one of the most prominent and useful statistics and we try to recover this power spectrum using the found estimator. The process of recovering the convergence power spectrum shown in figure 2 consists of two steps: First recovering the κ-values, which was explained in section 4.2, and second using these values to create a map and recovering the power spectrum from this recovered κ-map. Other recovered summary statistics such as the mean or the standard deviation are simply calculated from the convergence value distribution.

The recovery of the convergence map explained in section 4.2 results in a map with a sharp edge between the part covered by the catalogue and the rest. This creates problems in the recovery of the power spectrum. A solution is to smooth the mask – the map with ones in the covered part and zeros for the rest – before weighing our recovered convergence map with this mask. The power spectrum of this recovered convergence map is then calculated using the healpy anafast method [10].

5 Results

5.1 Estimators

As described in section 4.1, we use multiple ways to derive an estimator for the convergence κ. The results of these methods can be seen in figure 5 and they are all calculated for the largest catalogue with roughly $30,000,000$ galaxies over an area of 1000deg^2. Since equation 1 shows a linear relation between the galaxy sizes and κ, we will use a linear fit for the estimators. The corresponding fitted estimator per method can also be seen in the plots. We use an nside of 64 for the convergence map, for which reasons are shown in section 5.2. The theory for the mean has been calculated by using the mean of the catalogue and magnifying it with the corresponding κ-value. In total this means:

$$\theta_{\text{theory}} = \theta_{\text{catalogue mean}} \cdot (1 + \kappa) \tag{5}$$

This is used as the reference value, since ideally the unlensed mean of every pixel should be the same as the mean of the catalogue. That is why we can also use the unlensed mean as a measure if the number of galaxies per pixel is sufficient, more about that in section 5.2
Since we simulate galaxies on only a fraction of the sky, there are convergence map pixels that are only partially covered by the galaxy catalogue, so there are less galaxies in them than in the filled pixels. To increase the accuracy of the estimator, we need to have as many galaxies in a pixel as possible. This is why these border pixels are left out in the fitting of the estimator by introducing a galaxy number threshold. In most cases we will use a threshold of $20,000$ galaxies, but it varies depending of the resolution of the convergence map, which is further explained in section 5.2.
We also correct for too large galaxies, since they also have an impact on the mean and the Wasserstein distance, by introducing a size threshold of 5arcsec, which affects only very few galaxies, but includes outliers from the galaxy size sampling.

The first estimator plot seen in figure 5a shows the κ-values plotted against the means of the lensed (blue) and unlensed (red) sizes of all galaxies in a pixel. The black curve describes the theory seen in equation 5 and the green curve is the fitted estimator. The errors of the lensed means are the corresponding standard errors given by $\sigma_{\text{mean}} = \frac{\sigma}{\sqrt{N}}$, where σ is the standard deviation of the size destribution of the corresponding pixel, and N is the number of galaxies in the pixel. The next plot, figure 5b, shows the medians of the unlensed sizes again in red and in green the median of the lensed sizes. On the x-axis are again the κ-values of the pixels. The black curve describes the fitted estimator. It is similar for the third plot, figure 5c. Here the modes of the unlensed sizes, again red, and the lensed sizes, in grey, are plotted as a function of the κ-values of the pixels. The last plot shown in figure 5d shows the W1-Distance between the size distribution of one pixel to the size distribution of the whole catalogue as a function of the κ-values.

It is visible, that only the means show a theory curve. This is the case since it is the only case where the theoretical value can be calculated easily. For the other cases, since the size distribution for the galaxy sizes is rather complicated, it is complex to find a theoretical curve.
Another issue visible is the lack of an estimator fit for the modes. We refrained from fitting a linear relation onto the data since the scattering of the unlensed modes in comparison to the lensed modes is very large, so it is not possible to extract any information about the convergence κ from the modes.
Looking at the last method, the Wasserstein distance, it is clear that the gap in the middle looks unnatural. To understand this gap we have to look at the Wasserstein distance a bit closer. In general, the W1 distance is symmetric, this means that normally you could not decide if the κ-value if negative or positive. To fix this issue we also looked at the mean of the pixel. If the mean of the pixel is smaller than the mean of the catalogue, the sign of the κ-value is flipped, if it is larger, it stays the same. This method is not perfect, but serves as an easy way to overcome the sign problem. A problem that stays is this gap, since the W1 distance only becomes zero if the samples are exactly equal and not just statistically the same. This means, that it is more or less impossible to measure a very small κ-value using the W1 distance estimator. Using more galaxies per pixel shortens the gap, but in general the shape of the distribution stays the same.

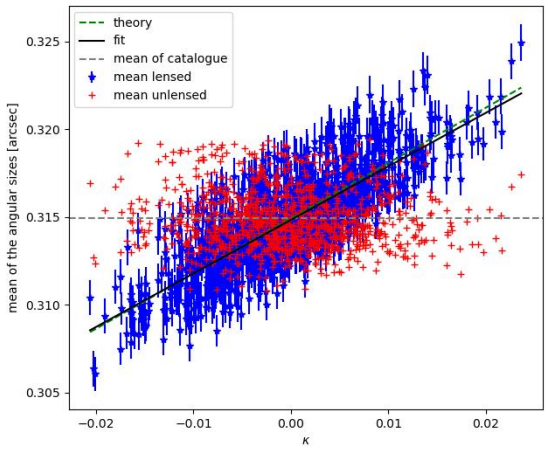

(a) Mean

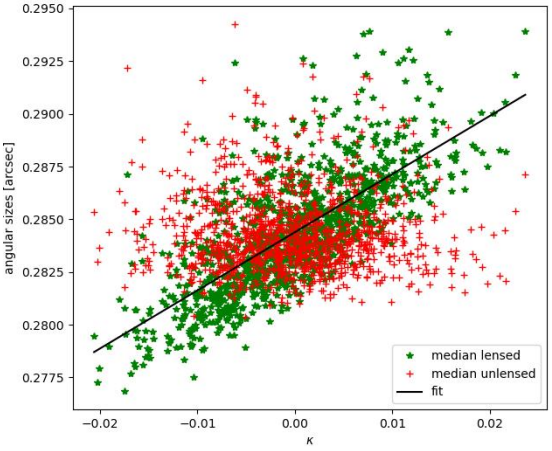

(b) Median

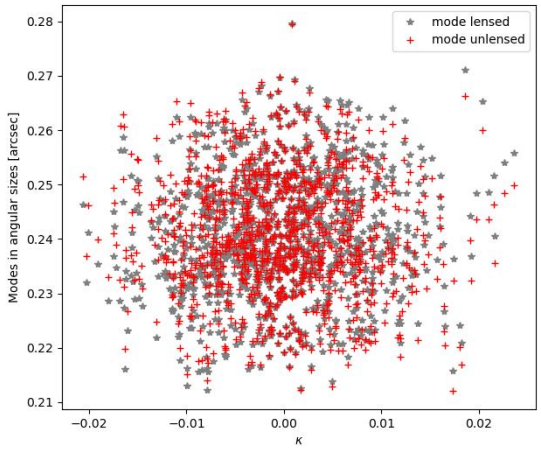

(c) Mode

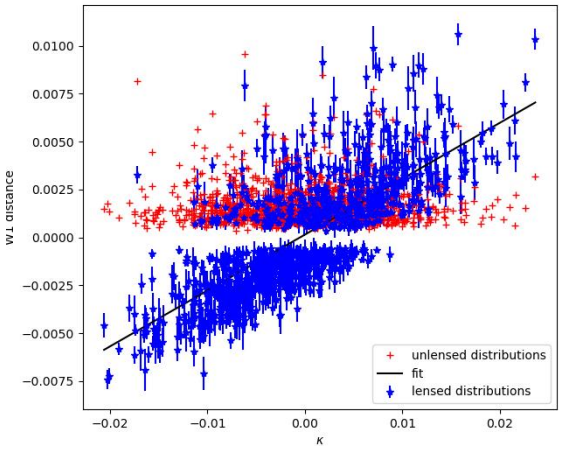

(d) W1 distance

Figure 5: The convergence estimators explored in this work. In each panel, the measured statistic (as stated under each plot) for the single pixels is plotted against the input convergence value (blue ,green or grey). We show the corresponding unlensed values in red. The derived estimators are plotted as a black curve and theory curves are plotted as a green dashed line. The errors for the means are the corresponding standard errors and for the W1 distance they are the standard deviation from the same calculations on a varied catalogue using a bootstrap. The grey dashed line in the panel of the means marks the mean of the whole catalogue.

The plots shown in figure 5 show various fitted estimators, but to use them to calculate κ from a given size distribution of a pixel, we still need to invert them. Since all of the fits are linear due to the linear relation seen in equation 1, the inverted function is given by the slope m and the y-intersect b of the fits via:

$$\kappa = \frac{1}{m} \cdot \mu - \frac{b}{m} \tag{6}$$

where μ is the calculated statistic of the size distribution, in this case the mean or the W1-distance.
Since the mean and the median show similar results and they also represent a similar idea, but it is far easier to work with the mean, we decided to not use the median any further but to concentrate on the mean and the Wasserstein distance. To compare the goodness of the two fits we calculated the respective R^2-value. The results are:

$$R^2_{\text{means}} = 0.83 \pm 0.19 \tag{7}$$

$$R^2_{\text{W1}} = 0.83 \pm 0.16 \tag{8}$$

The errors in equations 7 and 8 are the standard deviation of the R^2-value for varied catalogues using a bootstrap. The convergence map was left unchanged in the process.

5.2 Required galaxy numbers

As already mentioned, ideally all pixels would have the same unlensed mean as the whole catalogue, but of course this not the case since we only use a finite number of galaxies, which means that the unlensed means of the pixels also scatter around the catalogue mean. This can for example be seen in figure 5a, where the red dots, which show the unlensed means of the pixels, scatter around the catalogue mean, seen as the middle grey dashed line. To understand the behavior of this scattering better we simulate different

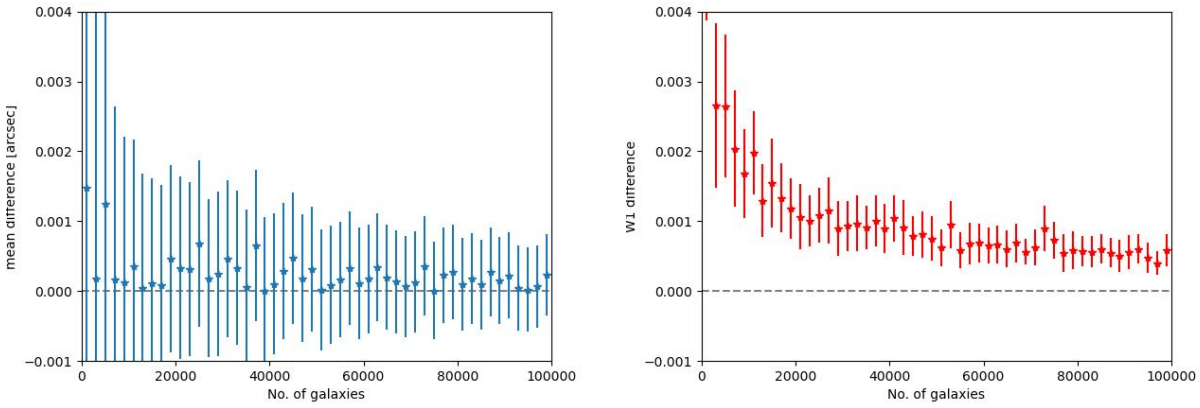

Figure 6: The absolute difference between the mean of the catalogue and a subset contained in one pixel and the W1 distance between the size distribution of the catalogue and the corresponding distribution of the pixel are shown in the left and right panel respectively. The simulated pixel is filled with different numbers of random galaxies which are visible on the x-axis, completely ignoring their initial position. All errors are standard deviations of the same calculations for different equally sized subsamples of the whole catalogue.

pixels with different numbers of galaxies by filling each pixel with the number of galaxies seen on the x-axis drawn at random from the catalogue. The result can be seen in figure 6. The errors seen in figure 6 are the standard deviation of the difference in the mean or the W1 distance of different samplings of the pixels for the different numbers of galaxies per pixel.
It is visible and also as we expected, that for larger numbers of galaxies per pixel, the scattering of the unlensed pixel means gets smaller. At roughly $15,000$ galaxies per pixel, the error of the mean and the W1 distance significantly drops and reaches a more or less constant level, so we would expect to get useful results at roughly $15,000$ galaxies per pixel or more. On the other hand, both plots show minor inconsistencies. The trend of the W1 distance scattering is also clearly going to zero, which is what we expect from a bootstrap error. The error furthermore never includes the zero line.

The next step now is to quantify the goodness of the fit for our estimators for different galaxy numbers per pixel. To do this we calculate the R^2-value for different numbers of galaxies per pixel. For this we simulate pixels filled with random galaxies in the catalogue ignoring their original position, apply the convergence map via 1 and calculate the R^2-value from the resulting estimator similar as in section 5.1.

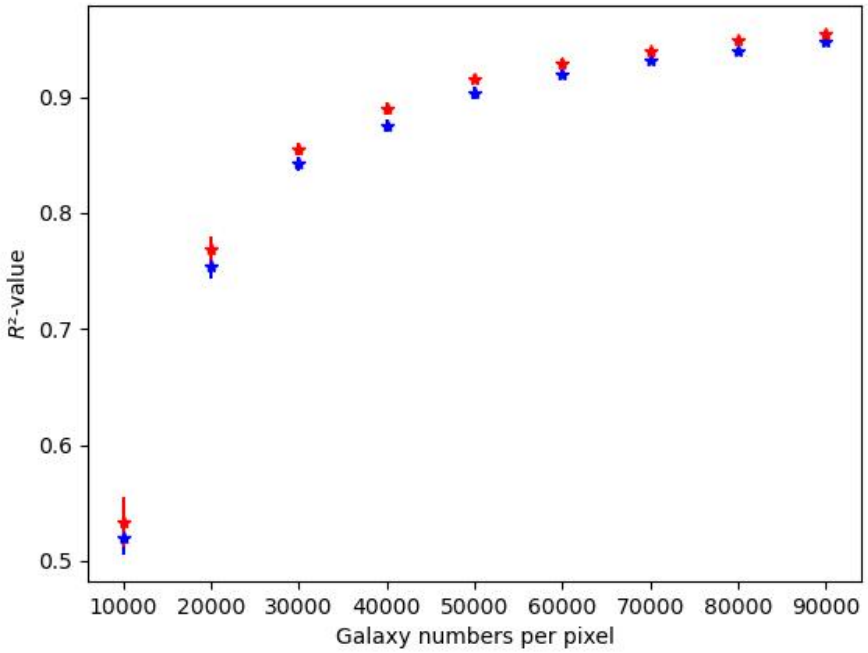

Figure 7: The R^2-values of the linear fit between input convergence and estimated pixelwise statistic for different galaxy numbers per pixel that have been drawn at random. In red the R^2-values of the estimator based on the W1 distance is shown and in blue the same for the estimator based on the means. The errors are standard deviations of the R^2-values calculated the same way for varied catalogues using a bootstrap.

As expected, the R^2-value gets closer to one for larger numbers of galaxies per pixel, for which the distributions should become more similar.

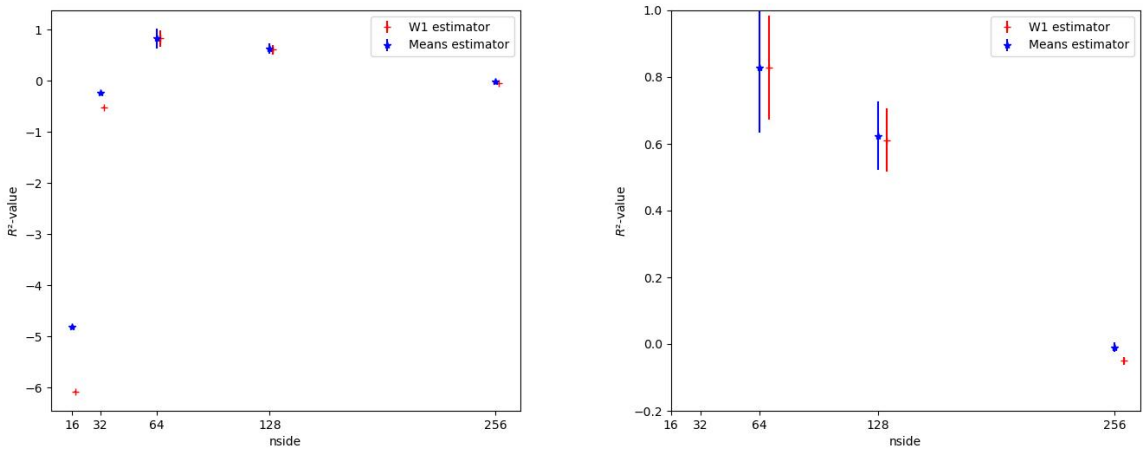

Figure 8: The R^2-values for different nsides of the convergence map. For a clearer visualization, we included an offset between the dots from the estimators based on the means and the W1-distance. Results for all nsides are shown in the left panel while the right panel shows only the largest three nsides. The errors show the standard deviation of the same calculation on varied catalogues using a bootstrap.

We can also calculate the R^2-value for different resolutions of the convergence map, so for different nsides. Now we also do not neglect the positions of the galaxies anymore, but the positions again determine the belonging of the galaxies to the pixels. The used galaxy number thresholds, introduced in section 5.1, are 274500, 76500, 20000, 5250, 1300 for the nsides 16, 32, 64, 128, 256 respectively, which is always roughly 80% of the average number of galaxies per pixel. The errors are again the standard deviation of the R^2-values calculated for varied catalogues using a bootstrap.
The plot shows, that only the nsides of 64 and 128 show significant errors. For the nsides 16 and 32 the errors align with figure 7, as the small nsides lead to large numbers of galaxies per pixel and figure 7 shows that the error gets smaller for large number of galaxies, but the value of the R^2 is significantly worse than for the other resolutions. This may be because there are too few pixels and therefore too few κ-values for a successful fit. Also, the R^2-values of nside 64 and the $20,000$ galaxies per pixel from figure 7 align, which is because the average number of galaxies for nside 64 is roughly $20,000$, so this is to be expected.
In retrorespect, this is the reason why we choose an nside of 64 for the calculation of the estimators. The average number of galaxies is above the needed threshold shown in figure 6, the R^2-value peaks at nside 64 in figure 8 and also because we need a high enough resolution to be able to recover summary statistics, which is done in the next section.

5.3 Recovery of convergence map

As already explained in section 4 we have two different methods for the recovery of the convergence map, but we will first focus on the first method, the pixelwise convergence recovery. The recoveries seen in this section have all been done multiple times for varied catalogues using a bootstrap. The original convergence map stays the same for all recoveries. All errors seen for the recovered summary statistics in this section are

the standard deviation of the different values for the varied catalogues.
To quantify the similarity between the recovered and the actual convergence maps we will look at several statistics, the first one being the mean of the convergence map. The convergence map is created such that its a Gaussian distribution with mean zero, which means the recovered maps should also have this property. The means of the κ-values per pixel for the different estimator methods are:

$$\bar{\kappa}_{\text{means}} = (-3.17 \pm 0.06) \cdot 10^{-4} \tag{9}$$

$$\bar{\kappa}_{\text{W1}} = (-7 \pm 6) \cdot 10^{-4} \tag{10}$$

The mean of the convergence map used for this calculation in the covered section of the catalogue has as mean of:

$$\bar{\kappa}_{\text{original}} = -3.9 \cdot 10^{-4} \tag{11}$$

This shows that all means of the distributions are close to zero, but only the values of the W1 distance and original mean align. The error of $\bar{\kappa}_{\text{means}}$ is also significantly smaller than the error of $\bar{\kappa}_{\text{W1}}$.

The standard deviations of the distributions are:

$$\sigma_{\text{means}} = (7.91 \pm 0.03) \cdot 10^{-3} \tag{12}$$

$$\sigma_{\text{W1}} = (8.5 \pm 0.6) \cdot 10^{-3} \tag{13}$$

$$\sigma_{\text{original}} = 7.3 \cdot 10^{-3} \tag{14}$$

The value of σ_{W1} is in a 2σ neighborhood of the original value, the value of σ_{means} on the other side does not align with the original value. In general both values of the recovered standard deviation are of the same magnitude as the original value.
Using the original power spectrum shown in figure 2, we are able to calculate the reference standard deviation of the κ distribution another way, by using equation 3 and modifying it into:

$$\sigma_\kappa = \sqrt{\sum_{l=0}^{\infty} \frac{2\ell + 1}{4\pi} C_\ell^\kappa} \tag{15}$$

The result by plugging in the original power spectrum is

$$\sigma_{\text{power spectrum}} = 7.25 \cdot 10^{-3} \tag{16}$$

where we only take the sum until $\ell = 3 \cdot \text{nside} - 1$, which is the highest ℓ which can be resolved by a given nside. The result is very similar to σ_{original}, which is also what we expect.

Next we can look at the so called one-point statistic, the distribution of the convergence map values. Since the used convergence map is Gaussian, the recovered map should also be Gaussian distributed. The histogram of the actual convergence map can be seen in figure 9. The corresponding histograms of the two recovered

convergence maps can be seen in figure 10. Since there are only just over 1000 pixels that cover the catalogue, the Gaussian distribution does not look perfect, even for the actual convergence map, but we investigate the true Gaussianity later in the section.

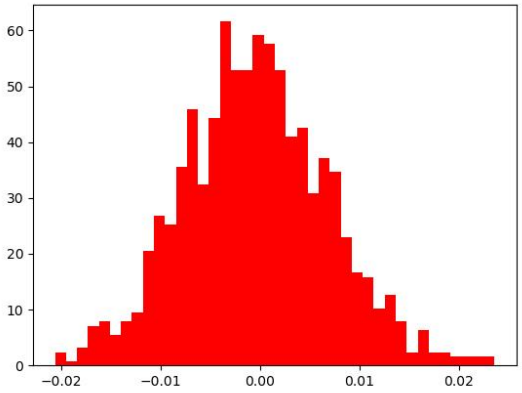

Figure 9: Histogram of the κ-values of the original convergence map in the section of the sky covered by the catalogue

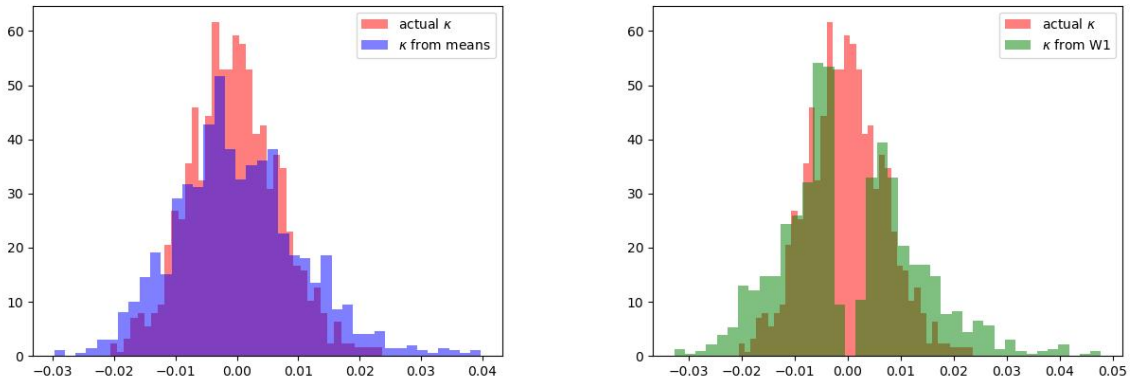

(a) Means

(b) W1 distance

Figure 10: Histogram of the κ-values of the recovered convergence map from the estimator using the means (left panel) and the W1 distance (right panel).

It is clearly visible that both distributions describe roughly a Gaussian and are roughly aligned with the distribution of the original κ-values. As seen in equation 13, the other distribution of the recovered map from the estimator using the W1 distance has a larger standard deviation as the distribution of the original convergence map, which is visible in figure 10b. As already seen before, all three distributions seem to have the same mean at around 0, which is also supported by the plotted distributions.
A way to quantify if the κ-values really describe a Gaussian is to compute the skewness of the distribution.

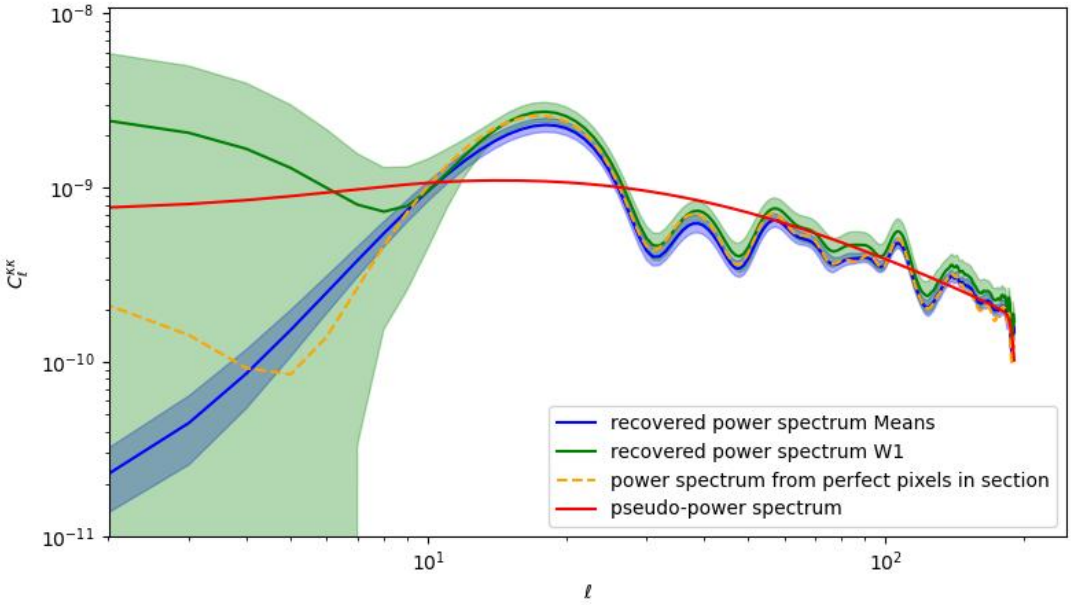

Figure 11: The recovered convergence power spectra for a pixelwise recovery of the convergence. The blue and green curve show the recovered power spectra from the estimator based on the means and W1 distance respectively while the shaded areas indicate the 1σ range calculated from doing the same recovery for varied catalogues using a bootstrap. The orange dashed line shows the recovered power spectrum of the original convergence map in the section covered by the catalogue.

For a Gaussian distribution this skewness must be 0, for the distributions the results of this computation are:

$$\gamma_{\text{means}} = 0.13 \pm 0.04 \tag{17}$$

$$\gamma_{\text{W1}} = 0.16 \pm 0.03 \tag{18}$$

$$\gamma_{\text{original}} = 0.16 \tag{19}$$

The skewness of the recovered convergence distributions based on the means and W1-distance both align with the skewness of the original convergence distribution.
To see if this is close enough to zero to validate our hypothesis we calculate the p-value of the null hypothesis, which is, the values are Gaussian distributed and the skewness is therefore zero. It describes the probability that the established phenomenon, a deviation from Gaussianity, does not exist, so it is the probability that the recovered κ-values are Gaussian distributed.

$$p_{\text{means}} = 0.11 \pm 0.09 \tag{20}$$

$$p_{\text{W1}} = 0.04 \pm 0.03 \tag{21}$$

$$p_{\text{original}} = 0.03 \tag{22}$$

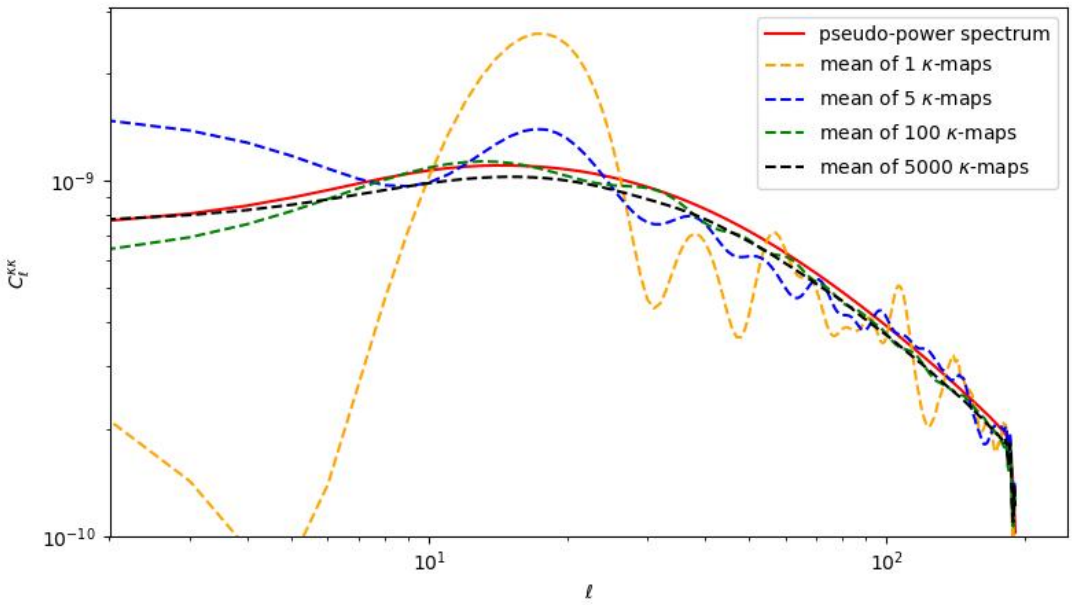

Figure 12: The mean of recovered power spectra of a masked convergence map in the section of the catalogue for different numbers of map realizations. The red curve shows the pseudo-power spectrum.

Normally 0.05 is picked as a threshold of significance, which only p_{means} surpasses. Since the original convergence values are definitely sampled from a Gaussian field, the p-value does not tell us much about the Gaussianity of the recovered distributions. The reason for the small p-values may be a result of the relatively small sample size of only roughly 1000 values.

Last we look at the power spectrum of the recovered convergence maps, they can be seen in figure 11. The blue and green curve show the recovered power spectrum from the estimators based on the means and on the W1-distance respectively. Before calculating the power spectrum, the map was smoothed as described in section 4.2.1 by multiplying them with a smoothed mask. In red the original power spectrum is shown, which was modeled forward, to factor in the influences of the mask, which is also known as the pseudo-power spectrum. It describes all the information that can be read out from the section covered by the catalogue and we will compare the results of the power spectrum recovery to this power spectrum. In orange, the recovered power spectra from the original κ-values is shown.

The recovered power spectra from the estimators both align well with the orange curve, the power spectrum of the original κ-values. The difference between the pseudo-power spectrum and the rest is probably because the rest only considers one realization of the original power spectrum shown in figure 2 as a convergence map. The red curve on the other hand is only dependent on the original power spectrum.
To verify that this is the reason for the difference, we calculate the mean of different power spectra, all recovered from one smoothed convergence map in the section covered by the catalogue. The result is shown

in figure 12. This shows that the recovered power spectrum gets closer to the pseudo-power spectrum when more samples of the convergence map are considered. Since in reality we are only able to measure one convergence map, this means there is a large uncertainty in the measurement. This is known as cosmic variance and its effect is primarily visible for small ℓ. An example of this can be seen in [1] for the power spectrum of the CMB.

The other method, the recovery of the convergence for every galaxy individually, was also implemented in the project but has not yet led to meaningful results.

6 Discussion

A big part of weak lensing studies is the investigation of the shear, the change of shape of galaxies. The counterpart, the change in size or the convergence, on the other hand has not been studied as extensively. In this project we try to find an estimator for the convergence. Using this estimator, we recover the underlying convergence power spectrum and other statistics.
We used different methods to find a suitable estimator, but the estimator based on the means and on the Wasserstein distance, shown in figure 5a and figure 5d respectively, are most promising. Both show clearly that there exists a signal which is not lost in the noise of the size scattering of the intrinsic size distributions. The recovery of the signal is limited by sampling noise, i.e. the number of galaxies per constant convergence pixel needs to be large enough. We show the limitations of our estimators (or limitations of the recovery of a signal) in section 5.2. One needs more than $15,000$ galaxies to ensure a robust recovery. This means that when applying our estimator to real observations and measuring the convergence power spectrum of the universe it is necessary to take at least this amount of galaxies into account in the calculation of the size distribution. A possible method of how to obtain an estimator for real observations, where the correlation length of the convergence field is unknown a priori, is explained in section 4.2.2, but has not yet lead to meaningful results. Regarding the pixelwise recovery method described in section 4.2.1, both the mean and the one-point statistic recovery are successful. The means of all three κ-value distributions, the original and the two recovered ones, are all close to zero as expected, but only the values of $\bar{\kappa}_{\mathrm{W1}}$ and $\bar{\kappa}_{\mathrm{original}}$ align within 1σ. The same holds for the standard deviations, where σ_{W1} and $\sigma_{\mathrm{original}}$ are in a 2σ neighborhood. The skewness γ of all three distributions align and are close to zero, which is to be expected from a Gaussian distribution. Lastly, the power spectra of the recovered convergence maps using the estimators both align with the power spectrum of the original κ-values in the section covered by the catalogue. For higher ℓ, they also roughly align with the pseudo-power spectrum. The differences between this pseudo-power spectrum and the other three power spectra comes from the fact that the three power spectra recovered from the convergence map are only measured on one realization of the convergence map. In reality we are also only able to measure the convergence map and then to recover the power spectrum from this, which is why we are only able to measure the power spectrum up to this uncertainty known as cosmic variance.

7 Outlook

Based on the results of this project, there are multiple paths that would be interesting to follow. Of course the most natural one is to follow the method described in section 4.2.2 to derive a robust way to measure the correlation function of the convergence. That this might be possible with enough data is shown in this project. One could also try out other methods to derive an estimator for the convergence, for example the maximum mean discrepancy might be promising. Another path worth following would be to look at simulated images which can also be generated by the package introduced in [4], where problems in the size measurement could come up. One could also use the measured power spectrum to infer cosmological parameters, as the power spectrum can be analytically described using these parameters.

References

[1] N. Aghanim et al. "Planck2018 results: V. CMB power spectra and likelihoods". In: *Astronomy amp; Astrophysics* 641 (Sept. 2020), A5. ISSN: 1432-0746. DOI: 10.1051/0004-[]6361/201936386. URL: http://dx.doi.org/10.1051/0004-[]6361/201936386.

[2] Matthias Bartelmann and Matteo Maturi. *Weak gravitational lensing*. 2016. arXiv: 1612.06535 [astro-ph.CO]. URL: https://arxiv.org/abs/1612.06535.

[3] A. S. Eddington. "The total eclipse of 1919 May 29 and the influence of gravitation on light". In: *The Observatory* 42 (1919), pp. 119–122.

[4] Silvan Fischbacher et al. *GalSBI: Phenomenological galaxy population model for cosmology using simulation-based inference*. 2025. arXiv: 2412.08701 [astro-ph.CO]. URL: https://arxiv.org/abs/2412.08701.

[5] Rémi Flamary et al. "POT: Python Optimal Transport". In: *Journal of Machine Learning Research* 22.78 (2021), pp. 1–8. URL: http://jmlr.org/papers/v22/20-[]451.html.

[6] D. Nelson Limber. "The Analysis of Counts of the Extragalactic Nebulae in Terms of a Fluctuating Density Field." In: 117 (Jan. 1953), p. 134. DOI: 10.1086/145672.

[7] Veronika Oehl. "Gravitational Lensing in the Light of Raychaudhuri's Equations and the Impact of Lensing on galaxy Size Distributions". MA thesis. University of Heidelberg, 2020.

[8] D. Walsh, R. F. Carswell, and R. J. Weymann. "0957 + 561 A, B - Twin quasistellar objects or gravitational lens". In: *Nature* 279 (1979), pp. 381–384. DOI: 10.1038/279381a0.

[9] Angus H. Wright et al. *KiDS-Legacy: Cosmological constraints from cosmic shear with the complete Kilo-Degree Survey*. 2025. arXiv: 2503.19441 [astro-ph.CO]. URL: https://arxiv.org/abs/2503.19441.

[10] Andrea Zonca et al. "healpy: equal area pixelization and spherical harmonics transforms for data on the sphere in Python". In: *Journal of Open Source Software* 4.35 (Mar. 2019), p. 1298. DOI: 10.21105/joss.01298. URL: https://doi.org/10.21105/joss.01298.